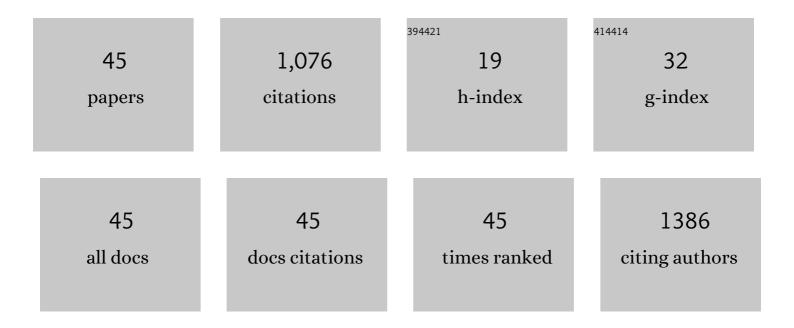
Michael Verrall

List of Publications by Year in descending order

Source: https://exaly.com/author-pdf/1574935/publications.pdf Version: 2024-02-01



#	Article	IF	CITATIONS
1	Morphology, composition and dissolution of chromite in the Goro lateritic nickel deposit, New Caledonia: Insight into ophiolite and laterite genesis. Ore Geology Reviews, 2022, 143, 104752.	2.7	2
2	Impact of prolonged waterâ€gas flow on the performance of polyacrylamide. Journal of Applied Polymer Science, 2022, 139, .	2.6	3
3	Mesozoic Hydrothermal Overprint on Carboniferous Bauxite in China. Economic Geology, 2021, 116, 787-800.	3.8	9
4	Sample preparation for rock wettability studies via atomic force microscopy. APPEA Journal, 2021, 61, 216.	0.2	1
5	Further Insights into the Performance of Silylated Polyacrylamide-Based Relative Permeability Modifiers in Carbonate Reservoirs and Influencing Factors. ACS Omega, 2021, 6, 13671-13683.	3.5	6
6	Reaction Coronas at Olivine–Plagioclase Contacts in Host Rocks from the Nova–Bollinger Ni–Cu–Co Deposit, Albany–Fraser Orogen, Western Australia: Evidence of a Magmatic to Metamorphic Continuum. Journal of Petrology, 2021, 62, .	2.8	9
7	Interface Sampling and Indicator Minerals for Detecting the Footprint of the Lancefield North Gold Deposit under the Permian Glacial Cover in Western Australia. Minerals (Basel, Switzerland), 2021, 11, 1131.	2.0	2
8	Mineralogy and geochemistry of atypical reduction spheroids from the Tumblagooda Sandstone, Western Australia. Sedimentology, 2020, 67, 677-698.	3.1	2
9	Formation water geochemistry for carbonate reservoirs in Ordos basin, China: Implications for hydrocarbon preservation by machine learning. Journal of Petroleum Science and Engineering, 2020, 185, 106673.	4.2	18
10	Life on the edge: Microbial biomineralization in an arsenic- and lead-rich deep-sea hydrothermal vent. Chemical Geology, 2020, 533, 119438.	3.3	10
11	A Multiscale Investigation of Cross-Linked Polymer Gel Injection in Sandstone Gas Reservoirs: Implications for Water Shutoff Treatment. Energy & Fuels, 2020, 34, 14046-14057.	5.1	17
12	Replacement reactions of copper sulphides at moderate temperature in acidic solutions. Ore Geology Reviews, 2020, 123, 103569.	2.7	16
13	Alteration patterns linked to high-grade gold mineralization at the Wattle Dam deposit, Western Australia. Ore Geology Reviews, 2020, 125, 103471.	2.7	3
14	New insights into the genesis of IOCG deposits: From a case study of the Yinachang deposit in SW China. Ore Geology Reviews, 2020, 124, 103664.	2.7	4
15	Pore Structure Changes Occur During CO2 Injection into Carbonate Reservoirs. Scientific Reports, 2020, 10, 3624.	3.3	48
16	Effects of geochemical reactions on multi-phase flow in porous media during CO2 injection. Fuel, 2020, 269, 117421.	6.4	18
17	Changes in multi-phase flow properties of carbonate porous media during CO2 injection. APPEA Journal, 2020, 60, 672.	0.2	0
18	X-ray micro-computed tomography and ultrasonic velocity analysis of fractured shale as a function of effective stress. Marine and Petroleum Geology, 2019, 110, 472-482.	3.3	23

MICHAEL VERRALL

#	Article	IF	CITATIONS
19	CO 2 â€Saturated Brine Injection Into Unconsolidated Sandstone: Implications for Carbon Geosequestration. Journal of Geophysical Research: Solid Earth, 2019, 124, 10823-10838.	3.4	10
20	Plundering Carlow Castle: First Look at a Unique Mesoarchean-Hosted Cu-Co-Au Deposit. Economic Geology, 2019, 114, 1021-1031.	3.8	8
21	Impact of Composition on Pore Structure Properties in Shale: Implications for Micro-/Mesopore Volume and Surface Area Prediction. Energy & Fuels, 2019, 33, 9619-9628.	5.1	37
22	Simulation and experimental measurements of internal magnetic field gradients and NMR transverse relaxation times (T2) in sandstone rocks. Journal of Petroleum Science and Engineering, 2019, 175, 985-997.	4.2	49
23	The Gove relict iron meteorite from Arnhem Land, Northern Territory, Australia. Meteoritics and Planetary Science, 2019, 54, 1710-1719.	1.6	23
24	An experimental study for carbonate reservoirs on the impact of CO2-EOR on petrophysics and oil recovery. Fuel, 2019, 235, 1019-1038.	6.4	50
25	A revised oxygen barometry in sulfide-saturated magmas and application to the Permian magmatic Ni–Cu deposits in the southern Central Asian Orogenic Belt. Mineralium Deposita, 2018, 53, 731-755.	4.1	48
26	Nanoscale geomechanical properties of Western Australian coal. Journal of Petroleum Science and Engineering, 2018, 162, 736-746.	4.2	40
27	Generation of amorphous carbon and crystallographic texture during low-temperature subseismic slip in calcite fault gouge. Geology, 2018, 46, 163-166.	4.4	15
28	CO2 saturated brine injected into fractured shale: An X-ray micro-tomography in-situ analysis at reservoir conditions. Energy Procedia, 2018, 154, 125-130.	1.8	3
29	Reactive Flow in Unconsolidated Sandstone: Application to Carbon Geosequestration. , 2018, , .		1
30	Pore characterization and clay bound water assessment in shale with a combination of NMR and low-pressure nitrogen gas adsorption. International Journal of Coal Geology, 2018, 194, 11-21.	5.0	138
31	The dynamics of gold in regolith change with differing environmental conditions over time. Geology, 2017, 45, 127-130.	4.4	16
32	Palaeobiology of red and white blood cell-like structures, collagen and cholesterol in an ichthyosaur bone. Scientific Reports, 2017, 7, 13776.	3.3	31
33	Excessive sulphur accumulation and ionic storage behaviour identified in species of <i>Acacia</i> (Leguminosae: Mimosoideae). Annals of Botany, 2016, 117, 653-666.	2.9	14
34	Poikilitic Textures, Heteradcumulates and Zoned Orthopyroxenes in the Ntaka Ultramafic Complex, Tanzania: Implications for Crystallization Mechanisms of Oikocrysts. Journal of Petrology, 2016, 57, 1171-1198.	2.8	55
35	Zirconolite, zircon and monazite-(Ce) U-Th-Pb age constraints on the emplacement, deformation and alteration history of the Cummins Range Carbonatite Complex, Halls Creek Orogen, Kimberley region, Western Australia. Mineralogy and Petrology, 2016, 110, 199-222.	1.1	27
36	Mineral exploration and basement mapping in areas of deep transported cover using indicator heavy minerals and paleoredox fronts, Yilgarn Craton, Western Australia. Ore Geology Reviews, 2016, 72, 485-509.	2.7	33

MICHAEL VERRALL

#	Article	IF	CITATIONS
37	Insights into the mechanics of en-échelon sigmoidal vein formation using ultra-high resolution photogrammetry and computed tomography. Journal of Structural Geology, 2015, 77, 27-44.	2.3	21
38	Stable H–C–O isotope and trace element geochemistry of the Cummins Range Carbonatite Complex, Kimberley region, Western Australia: implications for hydrothermal REE mineralization, carbonatite evolution and mantle source regions. Mineralium Deposita, 2014, 49, 905-932.	4.1	33
39	Biotite and Apatite as Tools for Tracking Pathways of Oxidized Fluids in the Archean East Repulse Gold Deposit, Australia. Economic Geology, 2013, 108, 667-690.	3.8	58
40	Preparation of Samples with Both Hard and Soft Phases for Electron Backscatter Diffraction: Examples from Gold Mineralization. Microscopy and Microanalysis, 2013, 19, 1007-1018.	0.4	12
41	Distribution of Metals in the Termite Tumulitermes tumuli (Froggatt): Two Types of Malpighian Tubule Concretion Host Zn and Ca Mutually Exclusively. PLoS ONE, 2011, 6, e27578.	2.5	37
42	Impact of grain-coating iron minerals on dielectric response of quartz sand and implications for ground-penetrating radar. Geophysics, 2011, 76, J27-J34.	2.6	6
43	Biological origin of minerals in pisoliths in the Darling Range of Western Australia. Australian Journal of Earth Sciences, 2011, 58, 823-833.	1.0	17
44	Mineralogy and crystal chemistry of "garnierites" in the Goro lateritic nickel deposit, New Caledonia. European Journal of Mineralogy, 2009, 21, 467-483.	1.3	77
45	Ionic gold in calcrete revealed by LA-ICP-MS, SXRF and XANES. Geochimica Et Cosmochimica Acta, 2009, 73, 1666-1683.	3.9	26